QCD measurements with jets and determinations of α_S at HERA

Krzysztof Nowak (for the H1 & ZEUS collaborations)
DESY, Notkestrasse 85, 22607 Hamburg, Germany
E-mail: krzysztof.nowak@desy.de

Abstract.
The *ep* collisions at HERA are a well suited environment for studying properties of perturbative QCD. Both the H1 and ZEUS collaborations present new jet measurements that span a wide Q^2 range, from photoproduction where $Q^2 \approx 0$ GeV^2 to Q^2 values of up to 20000 GeV^2. Inclusive jet, di-jet and tri-jet cross sections are generally well described by predictions of next-to-leading order QCD calculations. The measured cross sections are used to determine the strong coupling constant $\alpha_S(M_Z)$ and to test its predicted behaviour over a broad range of scales. HERA inclusive jet cross sections are also used in a QCD analysis for the precise simultaneous determination of parton density functions and $\alpha_S(M_Z)$.

1. Introduction

The HERA collider provides a very suitable environment for studying Quantum Chromodynamics (QCD). The H1 and ZEUS collaborations measure jet production in a wide range of the photon virtuality Q^2, starting from the region of photoproduction where Q^2 is very small up to Q^2 of few thousand GeV^2 in the deep-inelastic scattering (DIS) regime. The measurements provide an important test of current QCD calculations in next-to-leading order (NLO) of the strong coupling α_s and allow it's precise determination.

2. Jets in photoproduction

The exchanged photon in a photoproduction region (defined as $Q^2 < 1$ GeV^2) can be described as having two components: a direct and a resolved one. The direct component couples directly to a parton originating from the proton, while in the resolved case the photon first fluctuates into a $q\bar{q}$ pair (or an even more complex partonic state) and enters an interaction indirectly. The latter resembles hadron collisions as studied at the LHC. The ZEUS collaboration presents new preliminary inclusive jet [1] and di-jet [2] production results in the photoproduction region.

The inclusive jet results are based on data collected during the running period 2005 - 2006 with an integrated luminosity of 189 pb^{-1}. Jets with a transverse energy $E_T^{jet} > 17$ GeV were measured in the pseudorapidity range of $-1 < \eta^{jet} < 2.5$ within the kinematic range of $Q^2 < 1$ GeV^2 and inelasticity $0.2 < y < 0.85$. Results were compared to NLO QCD calculations obtained using the program by Klasen, Kleinwort and Kramer [3] with factorisation (μ_F) and renormalisation (μ_R) scales set to $\mu_R = \mu_F = E_T^{jet}$. Figure 1a presents the single differential jet cross sections $d\sigma/d\eta^{jet}$ compared to the theory predictions. The calculation reproduces the measured cross sections well everywhere, except for the most forward region of the phase space.

With the help of figure 1b, which presents the relative difference to the NLO prediction double differentially in pseudorapidity and transverse jet energy, the excess can be observed primarily at low jet energies.

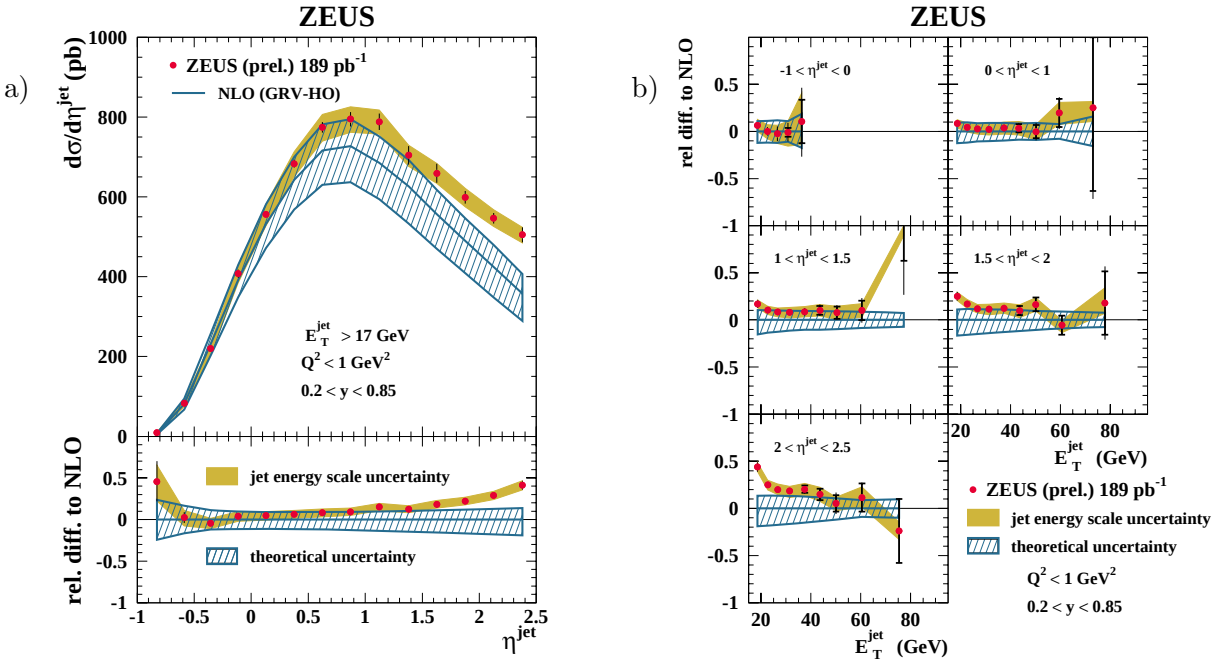

Figure 1. The single differential cross section $d\sigma/dE_T^{jet}$ (a) and the relative difference to the NLO prediction presented double differentially in η^{jet} and E_T^{jet} (b) for inclusive jet production in photoproduction as measured by the ZEUS collaboration [1].

A similar discrepancy was observed in previous ZEUS studies, where it was interpreted as an inadequacy of the poorly constrained photon PDFs [4] and a lack of non-perturbative (NP) effects such as the underlying events in the calculations [5]. The influence of the NP effects is investigated using the PYTHIA Monte Carlo generator and is presented in figure 2a. It is observed that correcting the NLO prediction for different assumptions on the NP effect leads to a larger jet rate at high η^{jet}, in the region where the NLO QCD calculation alone fails to describe the data. The difference between results obtained using alternative photon PDF sets is largest in the region where description by the NLO calculation is poor, as illustrated in the figure 2b.

The di-jet cross sections in photoproduction [2] are measured by the ZEUS collaboration in the phase space defined by $Q^2 < 1$ GeV^2, $0.2 < y < 0.85$, for transverse energies of the leading jet $E_T^{jet1} > 21$ GeV and of the sub-leading jet $E_T^{jet2} > 17$ GeV, in the jet pseudorapidity range $-1 < \eta^{jet} < 2.5$. Figure 3 presents the differential cross sections in bins of the average jet pseudorapidity $\bar{\eta}^{jet}$ and the fraction of the incoming photon momentum entering the hard interaction x_γ^{obs}. The results are compared to the NLO QCD prediction [3] with scales set to $\mu_R = \mu_F = E_T^{jet1}$ using several photon PDFs. In case of di-jet production the predictions provide a good description of the measurement.

Figure 4 summarises the relative theoretical uncertainties as a function of x_γ^{obs}. The uncertainty coming from the terms beyond NLO estimated by a variation of the scale by a factor of 2 up and down, is the main source limiting the precision of the calculation. In the region of low x_γ^{obs}, where resolved events dominate jet production, the uncertainty of the photon PDF is also significant.

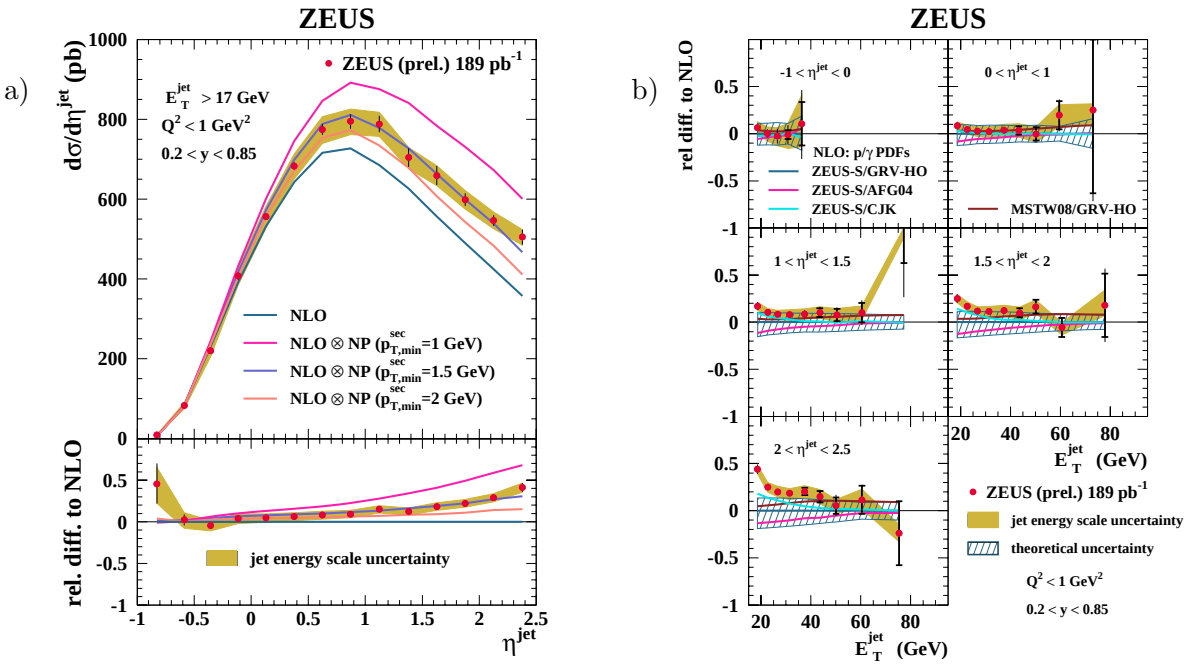

Figure 2. The inclusive jet production cross sections [1] $d\sigma/d\eta^{jet}$ in photoproduction compared to NLO QCD calculations including different estimates of non-perturbative effects (a) and the relative difference to NLO calculations using alternative photon PDF sets (b).

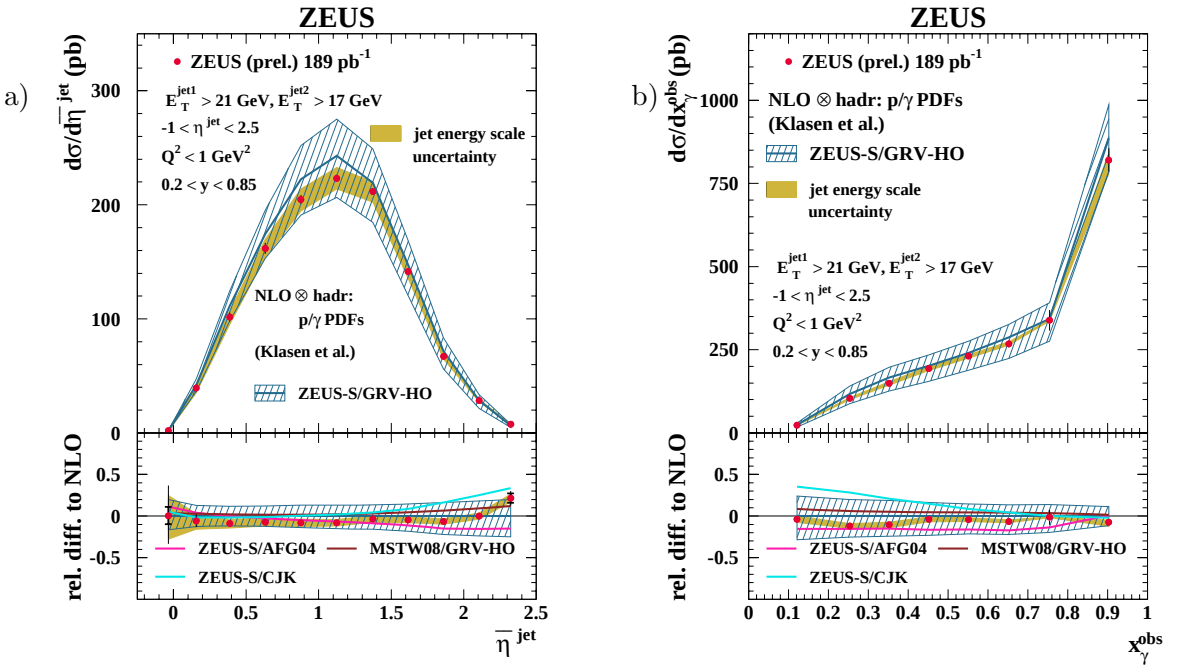

Figure 3. The di-jet cross sections in photoproduction [2] in bins of mean pseudorapidity $\bar{\eta}^{jet}$ (a) and x_γ^{obs} (b). The results are compared to predictions using alternative photon PDFs.

3. Jets in DIS

Both the H1 and ZEUS collaborations report several measurements of jet production in deep-inelastic scattering (DIS). While in photoproduction the jet energy is the natural choice for the

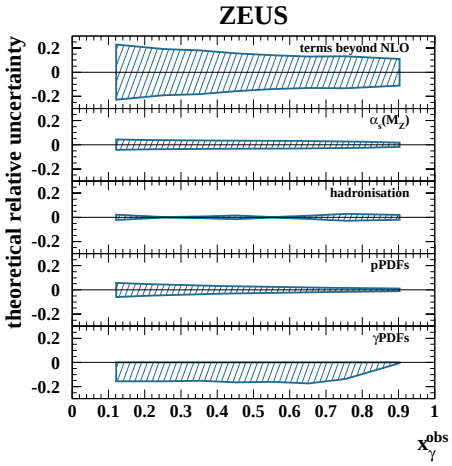

Figure 4. The relative theoretical uncertainty for the di-jet cross section prediction broken down into separate uncertainty sources as a function of x_γ^{obs} [2].

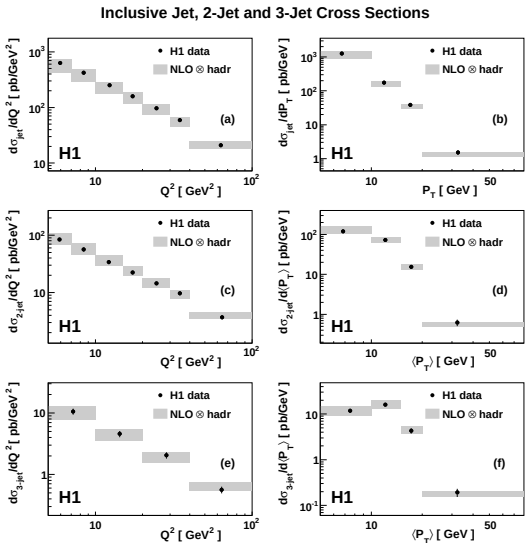

Figure 5. Inclusive jet (a, b), di-jet (c, d) and tri-jet (e, f) cross sections as a function of Q^2 and P_T or mean P_T in the low Q^2 DIS region as studied by H1 [6].

QCD scale, in DIS, Q^2 provides an additional or alternative hard scale. On the one hand that makes pQCD predictions reliable down to lower jet transverse energies, on the other hand, the choice of scale becomes more subtle. With increasing Q^2 the estimated theoretical uncertainty becomes smaller, which allows measurements in a phase space, where QCD calculations can provide results with reasonable accuracy.

The H1 collaboration measured inclusive and multijet cross sections in the low Q^2 DIS region [6]. Jets in a Breit frame with transverse energies $E_T^{jet} > 5$ GeV and within the pseudorapidity range $-1.0 < \eta^{jet} < 2.5$ are selected in the kinematic range of $5 < Q^2 < 100$ GeV^2 and $0.2 < y < 0.7$. Inclusive jet, di-jet and tri-jet cross sections were measured. In case of di- and tri-jet measurements, the phase space is restricted to the region where the invariant mass of the two leading jets M_{12} exceeds 18 GeV. This last requirement allows to avoid regions of phase space where fixed order theory is not reliable [7]. The results are based on data with integrated luminosity of 43.5 pb^{-1}.

Jet cross sections are predicted using the `NLOJET++` program [8] in next-to-leading order (NLO). The factorisation scale μ_F and the renormalisation scale μ_R are chosen to be $\mu_F = \mu_R = \sqrt{(Q^2 + P_{T,jet}^2)/2}$ which reflects the presence of two hard scales for jet production in DIS. This is of particular importance when both scales are comparable.

Figure 5 presents the cross sections in bins of Q^2 and jet transverse energy (mean transverse energy of the two leading jets in case of di- and tri-jet cross sections). One can note that the theoretical uncertainty, reaching 30% for the lowest Q^2 and P_T bins, limits the comparison and the high experimental precision of the data cannot be fully explored. Figure 6 presents the ratio of tri-jet to di-jet cross sections which benefits from cancellation of some experimental errors and, more importantly, shows a highly reduced sensitivity to the renormalisation scale variation. All results are consistent within errors with the calculations.

Complementary to the measurement in the low Q^2 range, results on jet production in the

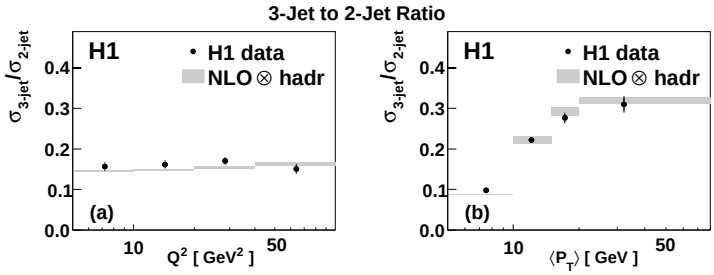

Figure 6. Ratios of tri-jet to di-jet cross sections as a function of Q^2 and $\langle P_T \rangle$ for the low Q^2 DIS jet measurement [6] compared to the NLO calculation.

high Q^2 region are presented by the H1 [9] and ZEUS [10, 11] collaborations. The new H1 analysis is based on data corresponding to an integrated luminosity of 351 pb^{-1} and studies jets in the kinematic region of $150 < Q^2 < 15000$ GeV^2 and $0.2 < y < 0.7$. Jets in the Breit frame with transverse momentum $7 < P_T^{jet} < 50$ GeV were measured in the pseudorapidity region of $-1.0 < \eta^{jet} < 2.5$. For di-jet and tri-jet measurements the minimal transverse momentum requirement is decreased to $P_T^{jet} > 5$ GeV, but an additional requirement on the invariant mass of the two leading jets $M_{12} > 16$ GeV is introduced for the same reason as explained above for jets in the low Q^2 region.

Due to the relatively high statistics of jets available at HERA and a well understood detector performance over the years, the hadronic energy scale uncertainty is usually the leading source of experimental error for HERA jet measurements. Recently, a large effort was undertaken by the H1 collaboration to improve the reconstruction and calibration of the hadronic final state (HFS). Figure 7 presents the mean value of the ratio of the transverse momentum of the HFS, P_T^h, to the reference scale P_T^{da}, the latter being independent of the calibration. At the bottom of figure 7 the double-ratio of data to MC is shown, which demonstrates the jet energy scale uncertainty of 1% over the whole studied phase space. The recent high Q^2 jet measurements profit from this improved jet calibration.

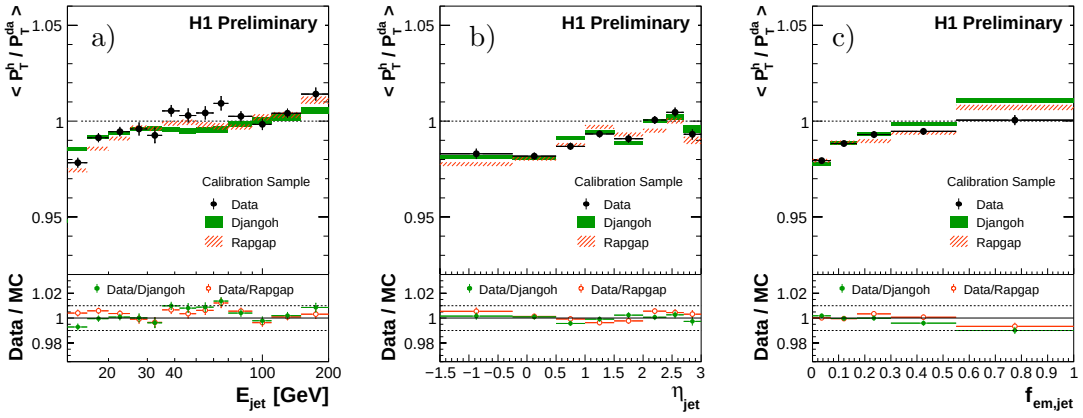

Figure 7. Ratio of the calibrated transverse momentum of the hadronic final state P_T^h to the reference measurement P_T^{da} as a function of the jet energy (a), jet pseudorapidity (b) and the fraction of jet energy deposited in the electromagnetic part of the calorimeter (c) as obtained with the recent H1 calibration [9].

Figure 8 presents preliminary inclusive, di-jet and tri-jet cross sections compared to the predictions calculated using the `NLOJET++` program [8] with the same choice of factorisation and renormalisation scales as in the case of the measurement in the low Q^2 region described above. The theory uncertainty, though lower than in the case of the low Q^2 DIS study, still

limits the comparison of the measurement to the prediction except at the highest Q^2 and highest energies, where experimental and theoretical uncertainties become comparable in size. The NLO prediction describes measured data well over the whole measured phase space.

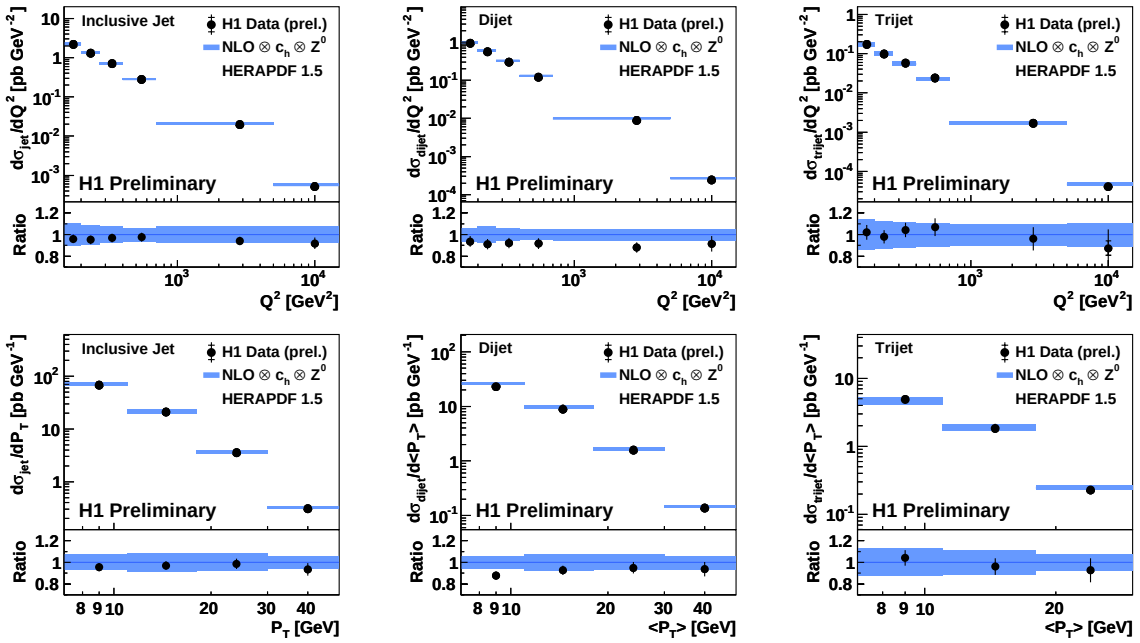

Figure 8. Differential cross sections $d\sigma/dQ^2$ and $d\sigma/dP_T$ for inclusive jet, di-jet and tri-jet production in the region of high Q^2 DIS by H1 [9].

Inclusive jet production at high Q^2 in DIS was studied also by the ZEUS collaboration [10]. The phase space of the measurement is given by $Q^2 > 125$ GeV^2 and $|\cos\gamma_h| < 0.65$. The angle γ_h corresponds in the quark-parton model to the direction of the scattered parton. Jets with $E_{T,jet}^{Breit} > 8$ GeV are selected in the range of pseudorapidity $-2.0 < \eta^{Breit} < 1.5$. The analysis is based on 300 pb^{-1} of HERA II data. Figure 9 presents the relative difference between measured cross sections and NLO calculation as a function of $E_{T,jet}^{Breit}$ in several regions of Q^2. The experimental and theoretical errors are comparable in size except at the very high $Q^2 > 5000$ GeV^2 where statistical errors dominate. The measurement is well described by the calculation over the whole studied phase space.

In addition to inclusive jet production, also di-jet production was studied by the ZEUS collaboration [11]. The measurement is based on the full HERA I and HERA II data corresponding to an integrated luminosity of 374 pb^{-1}. The phase space of the measurement is $125 < Q^2 < 20000$ GeV^2 and $0.2 < y < 0.6$. Jets are studied in the pseudorapidity range of $-1.0 < \eta^{LAB} < 2.5$ with transverse energies $E_{T,jet}^{Breit} > 8$ GeV. The invariant mass of the di-jet system is required to be $M_{jj} > 20$ GeV in order to ensure infrared safety of the theory calculations. The NLO calculation is provided by `NLOJET++` [8] with the factorisation scale $\mu_F = Q$ and renormalisation scale $\mu_R = \sqrt{Q^2 + \overline{E_T^{jet}}^2}$ where $\overline{E_T^{jet}}$ is the mean transverse energy of the two selected jets. Although H1 and ZEUS use different scales for the NLO calculation, both scale choices describe measurements well. For the ZEUS measurement this can be seen in figure 10, which presents the double differential cross sections as a function of Q^2 and $\log_{10}\xi$. Here ξ denotes the fraction of the proton momentum taken by the interacting parton estimated

as $\xi = x_{Bj}(1 + (M_{jj}^2/Q^2))$. The measurement is also compared to NLO predictions with other choices for μ_R and $\mu_R = \overline{E_T^{jet}}$ undershoots the data at low ξ in the highest Q^2 bin.

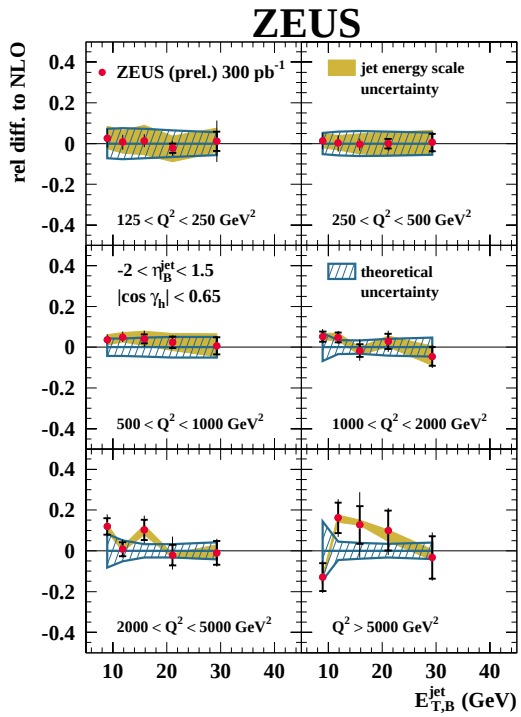

Figure 9. Relative difference of the differential inclusive jet cross sections $d\sigma/dE_T$ in bins of Q^2 to the NLO predictions [10].

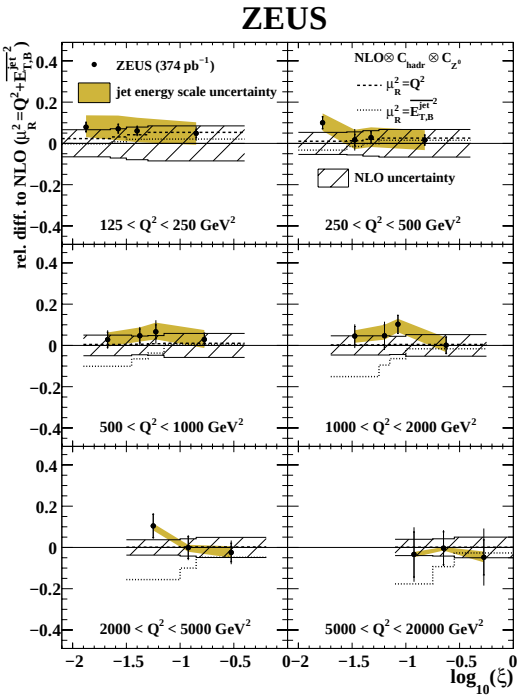

Figure 10. Relative difference of the differential di-jet cross sections $d\sigma/d\log_{10}\xi$ in bins of Q^2 to the NLO predictions [11].

To summarise, several recent jet production cross section measurements were presented, performed by both the H1 and ZEUS collaborations spanning a wide range of Q^2, from measurements in photoproduction where $Q^2 \approx 0$ GeV^2 to Q^2 values of up to 20000 GeV^2. No significant discrepancy between theory and measured data is observed, which increases the confidence in our good understanding of the QCD processes in ep collisions.

4. Jet algorithms comparison

The good understanding of the QCD theory for jet production, as outlined in the previous section, together with a relatively clean collision environment of ep collisions provide a perfect setup for studying the influence of the jet algorithm on the QCD results. It has been demonstrated that in the HERA environment of ep collision the longitudinally invariant k_T cluster algorithm [12] is well suited for performing reliable and useful measurements. It is not optimal though for hadron-hadron collisions like those at the LHC. In order to optimise jet measurements at LHC, new algorithms were recently developed, like the anti-k_T [13] and the SIScone [14] algorithms. The ZEUS collaboration studied the performances and behaviour of these algorithms. The study is based on the measurement of inclusive jet production in high Q^2 DIS [15] as well as in photoproduction [16], both introduced in the previous section.

Figure 11 shows the results of this comparison based on the measurements performed with 82 pb^{-1} of HERA I data. All three algorithms provide a similar performance and the NLO calculation describes the measured data well but they differ in details. At the bottom of

figure 11a the hadronisation correction factors are shown. For readability, the correction factor for the analysis with the k_T algorithm is shifted in order to distinguish it from the very similar anti-k_T algorithm performance. On average the hadronisation correction factor differs from unity by about 6% for both the k_T and anti-k_T algorithms. The analysis based on the SIScone algorithm produces results that need a higher hadronisation correction of 11% on average.

The significance of different theoretical uncertainties is presented in figure 11b. The uncertainty coming from the terms beyond NLO, as estimated by variation of the renormalisation scale μ_r by a factor of 2 up and down, dominates the precision of the calculation. The SIScone algorithm is more sensitive to this variation, which results in a slightly higher total theoretical uncertainty.

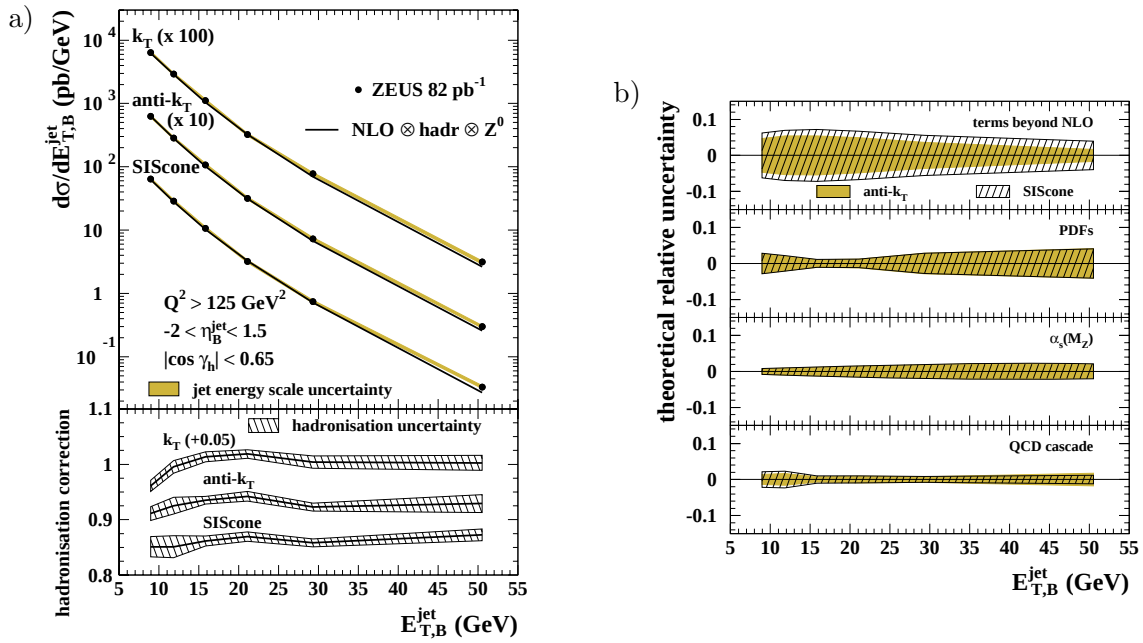

Figure 11. The differential inclusive jet cross sections $d\sigma/dE^{jet}_{T,B}$ and the hadronisation correction as a function of $E^{jet}_{T,B}$ using three different jet algorithms(a). The breakdown of theoretical uncertainties as estimated for the anti-k_T and SIScone algorithms (b) [15].

5. Determination of the strong coupling constant

The QCD predictions for jet production directly depend on the strong coupling constant $\alpha_S(M_Z)$ and the precisely determined cross sections can be used to extract its value. While the calculations of jet cross sections in NLO can take considerable time, the `FASTNLO` program [17] provides an efficient method to convolute matrix elements provided by `NLOJET++` with the PDFs and α_S. It is used to extract the best value of the strong coupling constant in the DIS region ([6, 9, 10]). The method of extracting $\alpha_S(M_Z)$ from photoproduction data is described in [1]. The values of the strong coupling obtained from the inclusive jet data are summarised in figure 12a. In addition to values obtained from jet cross sections presented in this document, the figure contains $\alpha_S(M_Z)$ extracted with the help of the normalised jet cross sections [18] published by the H1 collaboration, which remains experimentally most precise $\alpha_S(M_Z)$ value obtained at HERA. The theoretical part of the $\alpha_S(M_Z)$ uncertainty contains the effects coming from

the scale variation in the calculations as well as the uncertainty of our knowledge about PDFs and the hadronisation process. One may again note the relatively large theoretical uncertainty for the $\alpha_S(M_Z)$ determination based on the low Q^2 DIS phase space as compared to the high Q^2 region. This is the effect of the relatively low renormalisation scale as compared to the photoproduction measurement which is based on jets with higher transverse energies, as well as the measurements in the higher Q^2 range. Figure 12b presents the $\alpha_S(M_Z)$ values obtained from the fit to di-jet and tri-jet cross sections.

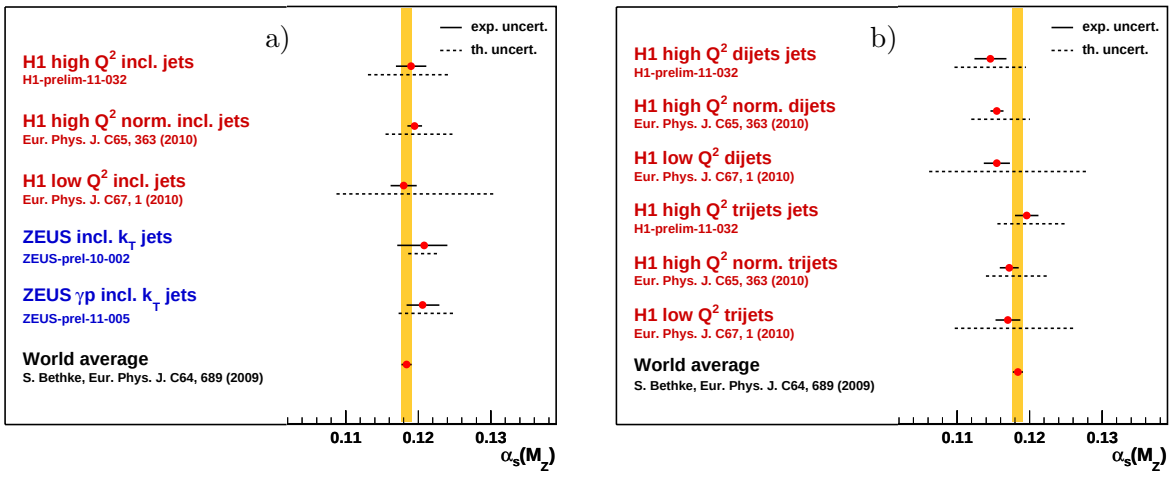

Figure 12. Summary of the strong coupling constants obtained from the H1 and ZEUS fit to the inclusive jet cross sections (a) as well as di-jet and tri-jet cross sections (b) compared to the world average $\alpha_S(M_Z)$ value [19].

The HERA experiments, having access to a wide range of scale values allow testing of theoretical prediction to the running of $\alpha_S(\mu_R)$. Figure 13 presents the extraction of α_S performed at different scales from both H1 and ZEUS. The obtained results are in good agreement with the predicted running of the strong coupling. They are also consistent with each other.

6. Simultaneous determination of PDFs and $\alpha_S(M_Z)$

H1 and ZEUS have released several sets of proton PDFs based purely on HERA data, called HERAPDF [20]. Generally, determination of PDFs is based on a χ^2 fit to the data with the strong coupling constant fixed to the value measured in other experiments (more precisely, to the world average [19] value of the strong coupling constant being an average value of many measurements from independent experiments and performed with a broad spectrum of methods). Recently the H1 and ZEUS collaborations presented a fit called HERAPDF1.6 [21] performed without a prior assumption on $\alpha_S(M_Z)$ which is fitted simultaneously with the PDFs.

The data used in the fit consists of the preliminary combined H1 and ZEUS charged and neutral current inclusive DIS cross sections [22] along with the H1 high Q^2 normalised inclusive jet cross sections [18], H1 low Q^2 inclusive jet cross sections [6], and two sets of ZEUS DIS inclusive cross sections [23, 24]. The calculations are performed with the NLOJET++ program [8], with factorisation and renormalisation scales set following the original publications.

Figure 14 presents a comparison of the PDFs obtained from the fits to inclusive DIS data only (HERAPDF1.5f) and to inclusive DIS and jet data simultaneously (HERAPDF1.6). In both cases $\alpha_S(M_Z)$ was treated as a free parameter in the fit. When fit is performed on inclusive DIS

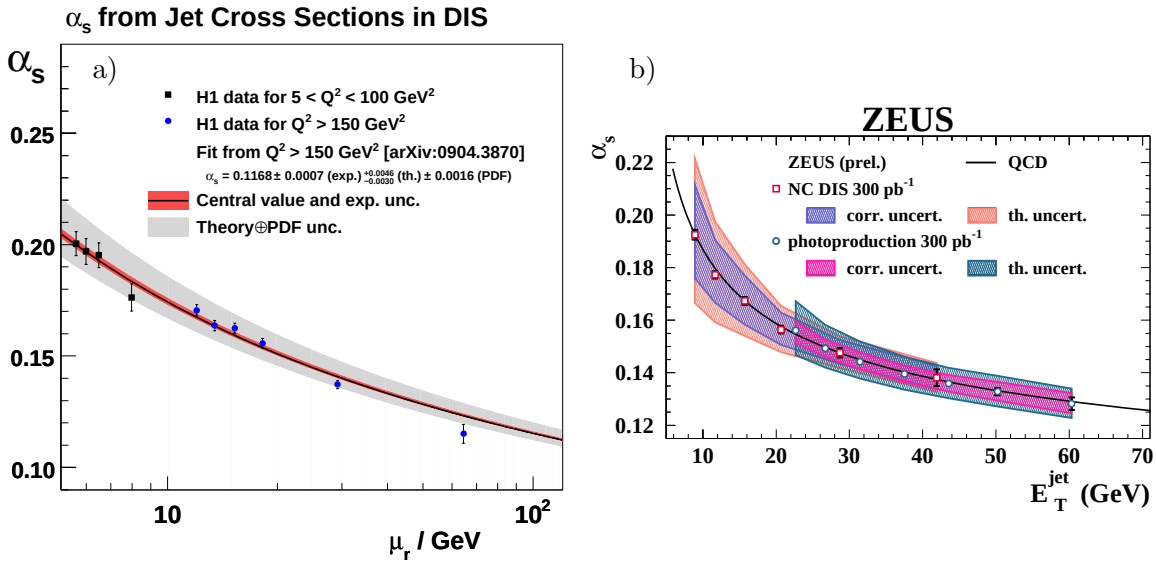

Figure 13. The evolution of α_S as a function of the renormalisation scale μ_r, comparing measurements in different regions of Q^2 from the H1 [6, 18] (a) and ZEUS [1, 10] (b) collaborations. The renormalisation scale for H1 measurements was chosen to be $\mu_R = \sqrt{(Q^2 + P^2_{T,jet})/2}$ while ZEUS collaboration assumed $\mu_R = E^{jet}_T$.

data only, it results in a gluon density function with considerably increased uncertainty. This is due to the high correlation between gluon PDF and the strong coupling constant. Inclusion of the HERA jet data in the fit significantly decreases this correlation and allows a precise simultaneous determination of PDFs and $\alpha_S(M_Z)$. The details of the method and the uncertainty evaluation are given in [20].

This effect can also be seen in the values of $\alpha_S(M_Z)$ obtained from the two fits. It is visualised in figure 15 by means of a χ^2 scan as a function of assumed values for $\alpha_S(M_Z)$. The fit without jet data exhibits a shallow χ^2 minimum, while the fit incorporating jet data produces a narrow minimum which allows a precise determination of $\alpha_S(M_Z)$. The value of $\alpha_S(M_Z)$ extracted from the HERAPDF1.6 fit is:

$$\alpha_S(M_Z) = 0.1202 \pm 0.0013(\text{exp}) \pm 0.0007(\text{model/param}) \pm 0.0012(\text{hadr})^{+0.0045}_{-0.0036}(\text{scale})$$

Here 'exp' means the experimental error, 'model/param' refers to the model and parametrisation uncertainty, 'hadr' to the hadronisation uncertainty and 'scale' stands for an estimation of the uncertainty coming from higher orders not included in the calculations employing the standard procedure of varying the renormalisation and factorisation scales by factor of 2 up and down. The obtained value of $\alpha_S(M_Z)$ is in good agreement with the values described in section 5 and with the world average [19].

7. Summary

Several new jet production measurements performed on data collected at the HERA *ep* collider by both the H1 and ZEUS collaborations were presented. Improvements in the precision were achieved by using the large HERA II statistics and on improved detector calibration. The measured cross sections were used for the extraction of the strong coupling constant $\alpha_S(M_Z)$ with very good experimental precision. The theoretical uncertainty on the extracted $\alpha_S(M_Z)$

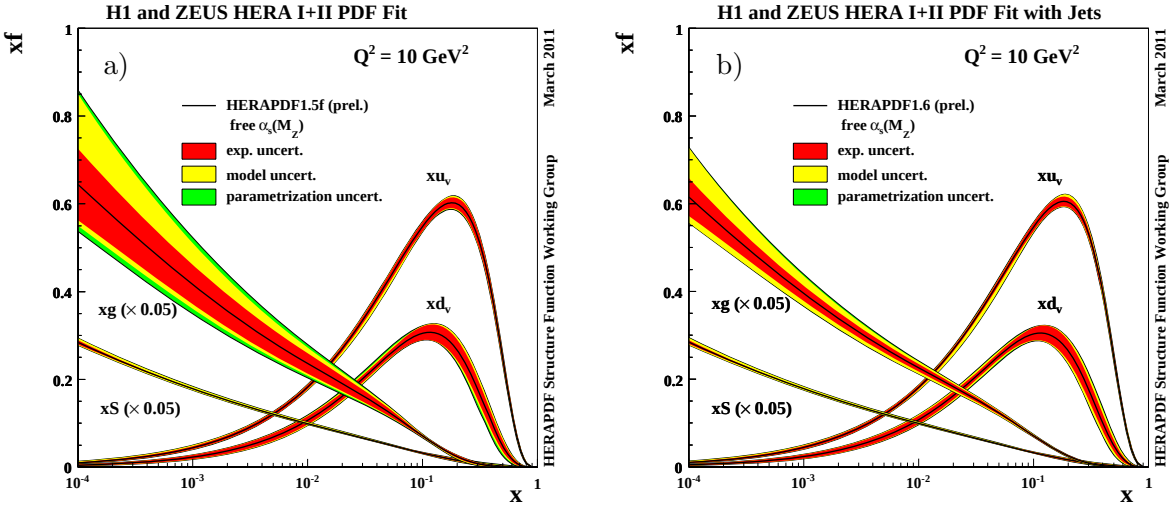

Figure 14. The parton density functions xu_v, xd_v, xS and xg at $Q^2 = 10$ GeV^2 as obtained from a fit to inclusive DIS data only (a) and to inclusive DIS and jet data simultaneously (b) with $\alpha_S(M_Z)$ treated as a free parameter of the fit. The experimental, model and parametrisation uncertainties are shown separately [21].

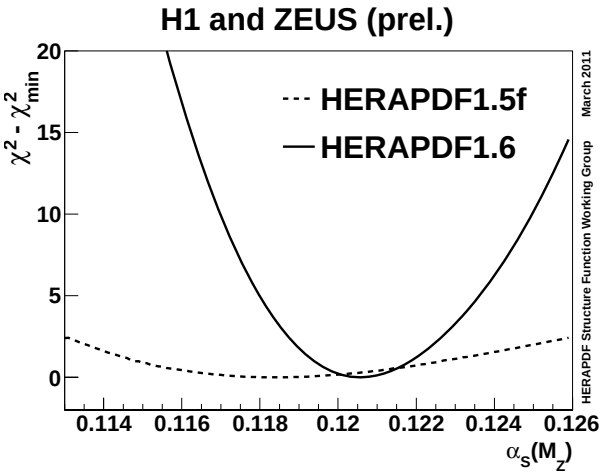

Figure 15. The difference between χ^2 and its minimum value for the fit to inclusive DIS data only (HERAPDF1.5f) and to inclusive DIS and jet data simultaneously (HERAPDF1.6) as a function of assumed $\alpha_S(M_Z)$ values [21].

value is large, dominated by the variation of the renormalisation scale, and the existence of NNLO calculations could further improve the achieved precision. The new jet measurements span over broad range of Q^2 starting from the photoproduction regime up to 20000 GeV^2, providing a unique opportunity to study the behaviour of the strong coupling α_S over a wide range of scales. Jet measurements are used together with the HERA inclusive DIS data in a QCD analysis for a simultaneous determination of the parton density functions and $\alpha_S(M_Z)$.

References

[1] Lontkovskyi D (ZEUS Collaboration) 2010 *PoS* **DIS2010** 120
[2] *ZEUS Collaboration, ZEUS-prel-10-014*
[3] Klasen M, Kleinwort T and Kramer G 1998 *Eur.Phys.J.direct* **C1** 1 (*Preprint* `hep-ph/9712256`)
[4] Chekanov S *et al.* (ZEUS Collaboration) 2007 *Phys.Rev.* **D76** 072011 (*Preprint* `0706.3809`)
[5] Chekanov S *et al.* (ZEUS Collaboration) 2008 *Nucl.Phys.* **B792** 1–47 (*Preprint* `0707.3749`)

[6] Aaron F *et al.* (H1 Collaboration) 2010 *Eur.Phys.J.* **C67** 1–24 (*Preprint* 0911.5678)
[7] Frixione S and Ridolfi G 1997 *Nucl.Phys.* **B507** 315–333 (*Preprint* hep-ph/9707345)
[8] Nagy Z and Trocsanyi Z 2001 *Phys.Rev.Lett.* **87** 082001 (*Preprint* hep-ph/0104315)
[9] *Kogler R (H1 Collaboration) Measurement of Multijet Production in Deep-Inelastic ep Scattering at HERA, proceedings of DIS 2011, Newport News, USA*
[10] Glasman C (ZEUS Collaboration) 2010 *PoS* **DIS2010** 107 (*Preprint* 1006.2342)
[11] Abramowicz H *et al.* (ZEUS Collaboration) 2010 *Eur.Phys.J.* **C70** 965–982 (*Preprint* 1010.6167)
[12] Catani S, Dokshitzer Y L, Seymour M and Webber B 1993 *Nucl.Phys.* **B406** 187–224
[13] Cacciari M, Salam G P and Soyez G 2008 *JHEP* **0804** 063 (*Preprint* 0802.1189)
[14] Salam G P and Soyez G 2007 *JHEP* **0705** 086 (*Preprint* 0704.0292)
[15] Abramowicz H *et al.* (The ZEUS Collaboration) 2010 *Phys.Lett.* **B691** 127–137 (*Preprint* 1003.2923)
[16] *ZEUS Collaboration, ZEUS-prel-10-015*
[17] Kluge T, Rabbertz K and Wobisch M 2006 483–486 (*Preprint* hep-ph/0609285)
[18] Aaron F *et al.* (H1 Collaboration) 2010 *Eur.Phys.J.* **C65** 363–383 (*Preprint* 0904.3870)
[19] Bethke S 2009 *Eur.Phys.J.* **C64** 689–703 (*Preprint* 0908.1135)
[20] Aaron F *et al.* (H1 and ZEUS Collaboration) 2010 *JHEP* **1001** 109 (*Preprint* 0911.0884)
[21] *H1 and ZEUS Collaborations, H1prelim-11-034, ZEUS-prel-11-001*
[22] *H1 and ZEUS Collaborations, H1prelim-10-142, ZEUS-prel-10-018*
[23] Chekanov S *et al.* (ZEUS Collaboration) 2002 *Phys.Lett.* **B547** 164–180 (*Preprint* hep-ex/0208037)
[24] Chekanov S *et al.* (ZEUS Collaboration) 2007 *Nucl.Phys.* **B765** 1–30 (*Preprint* hep-ex/0608048)